Arch Appl Mech (2008) 78: 587–597
DOI 10.1007/s00419-007-0178-1

ORIGINAL

K. C. Le · P. Sembiring

Analytical solution of plane constrained shear problem for single crystals within continuum dislocation theory

Received: 3 April 2007 / Accepted: 14 September 2007 / Published online: 19 October 2007

Abstract Berdichevsky and Le have recently found the analytical solution of the anti-plane constrained shear problem within the continuum dislocation theory (CMT, Contin. Mech. Thermodyn. 18:455–467, 2007). Interesting features of this solution are the energetic and dissipative thresholds for dislocation nucleation, the Bauschinger translational work hardening, and the size effect. In this paper an analytical solution of the plane constrained shear problem for single crystals exhibiting similar features is obtained and the comparison with the discrete dislocation simulation is provided.

Keywords Dislocations · Plane constrained shear · Thresholds · Work hardening · Size effect

1 Introduction

When crystalline solids deform plastically, newly formed dislocations pile up near the grain boundaries giving rise to material strengthening. Dislocations appear in the crystal lattice to reduce its energy. Motion of dislocations yields the dissipation of energy, which, in turn, results in a resistance to the dislocation motion. Any plasticity theory aiming at predicting plastic yielding, work hardening, and hysteresis must, therefore, take the nucleation and motion of dislocations into account. The continuum description of geometrically necessary dislocations is dictated by the high dislocation densities accompanying plastic deformations, which are in the range of 10^8–$10^{15}\,\mathrm{m}^{-2}$, as well as the complexity of the dislocation network. Although the framework of the continuum dislocation theory was laid down long time ago by Nye [1], Kondo [2], Bilby et al. [3], Kröner [4], and Sedov and Berdichevsky [5], among others, the applicability of the theory has become feasible only in recent years [6,7], thanks to the progress in statistical mechanics and thermodynamics of dislocation network [8,9]. Among various dislocation-based plasticity theories, we mention here only those in [10–14] which are closely relevant to our approach. In [15] the analytical solution of the anti-plane constrained shear problem was found. The interesting features of this solution are the energetic and dissipative yielding thresholds, the Bauschinger translational work hardening and the size effect. The dislocation nucleation admits a clear characterization by the variational principle for the final plastic states [6].

This paper deals with the plane-strain constrained shear of a strip made up of a single crystal. We aim at showing that, if only a single slip system is admitted, the analytical solution of this problem which exhibits the same features as that found in [15] is available. The comparison with the results of discrete dislocation simulations reported in [11,12] shows good agreement between the discrete and continuum approaches.

The paper is organized as follows. The setting of the problem is outlined in Sect. 2. Section 3 studies dislocation nucleation at zero resistance by energy minimization. In Sect. 4 the plastic distortion at nonzero

Dedicated to the memory of George Herrmann

K. C. Le (✉) · P. Sembiring
Lehrstuhl für Allgemeine Mechanik, Ruhr-Universität Bochum, 44780 Bochum, Germany
E-mail: chau.le@rub.de

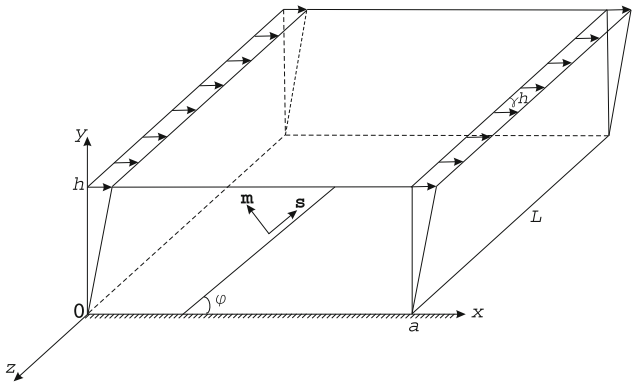

Fig. 1 Plane-strain constrained shear

resistance to dislocation motion is analyzed. Section 5 discusses the dislocation density, the Bauschinger translational work hardening and the size effect.

2 Plane-strain constrained shear

Consider the strip made up of a single crystal undergoing a plane-strain shear deformation (see Fig. 1). Let the cross-section of the strip be a rectangle of width a and height h, $0 \le x \le a$, $0 \le y \le h$. We realize the shear deformation by placing the strip in a "hard" device with the prescribed displacements at its upper and lower sides

$$u(0) = 0, \quad v(0) = 0, \quad u(h) = \gamma h, \quad v(h) = 0, \tag{1}$$

where $u(y)$ and $v(y)$ are the longitudinal and transverse displacements, respectively, with γ being the overall shear strain. The hard device models the grain boundary. We assume that the length of the strip L is very large and the width a is much greater than the height h ($L \gg a \gg h$) to neglect the end effects and to have the stresses and strains depending only on one variable y in the central part of the strip.

For the plane strain state, the components of the strain tensor are

$$\varepsilon_{xx} = 0, \quad \varepsilon_{xy} = \varepsilon_{yx} = \frac{1}{2}u_{,y}, \quad \varepsilon_{yy} = v_{,y}, \tag{2}$$

where the comma in indices denotes the derivative with respect to the corresponding coordinate. If the shear strain γ is sufficiently small, then the crystal deforms elastically and $u = \gamma y$, $v = 0$ everywhere in the strip. If γ exceeds some critical threshold, then edge dislocations may appear. We admit only the slip directions (or the directions of the Burgers vectors) perpendicular to the z-axis and inclined at an angle φ with the x-axis and the dislocation lines parallel to the z-axis. Since only one slip system is active, the plastic distortion is given by $\beta_{ij} = \beta s_i m_j$, with $s = (\cos\varphi, \sin\varphi)$ being the slip direction, and $m = (-\sin\varphi, \cos\varphi)$ the normal vector to the slip plane. We assume that β depends only on y: $\beta = \beta(y)$ (translational invariance). Because of the prescribed boundary conditions (1), dislocations cannot penetrate the boundaries $y = 0$ and $y = h$; therefore

$$\beta(0) = \beta(h) = 0. \tag{3}$$

The components of the plastic strain tensor $\varepsilon^p_{ij} = \frac{1}{2}(\beta_{ij} + \beta_{ji})$ are

$$\varepsilon^p_{xx} = -\frac{1}{2}\beta \sin 2\varphi, \quad \varepsilon^p_{xy} = \frac{1}{2}\beta \cos 2\varphi, \quad \varepsilon^p_{yy} = \frac{1}{2}\beta \sin 2\varphi. \tag{4}$$

With (2) and (4), we obtain the components of the elastic strain tensor $\varepsilon^e_{ij} = \varepsilon_{ij} - \varepsilon^p_{ij}$

$$\varepsilon^e_{xx} = \frac{1}{2}\beta \sin 2\varphi, \quad \varepsilon^e_{xy} = \frac{1}{2}(u_{,y} - \beta \cos 2\varphi), \quad \varepsilon^e_{yy} = v_{,y} - \frac{1}{2}\beta \sin 2\varphi. \tag{5}$$

As β depends only on y, there are two non-zero components of Nye's dislocation density tensor $\alpha_{ij} = \epsilon_{jkl}\beta_{il,k}$, namely, $\alpha_{xz} = \beta_{,y} \sin\varphi \cos\varphi$ and $\alpha_{yz} = \beta_{,y} \sin^2\varphi$. Thus, the resultant Burgers vector of all dislocations whose

dislocation lines cut the area perpendicular to the z-axis is parallel to the slip direction s and the scalar dislocation density equals

$$\rho = \frac{1}{b}\sqrt{\alpha_{ij}\alpha_{ij}} = \frac{1}{b}|\beta_{,y}||\sin\varphi|,$$

where b is the magnitude of the Burgers vector.

Energy per unit volume of the crystal with dislocations reads [9,6]

$$U(\varepsilon^e_{ij}, \alpha_{ij}) = \frac{1}{2}\lambda\left(\varepsilon^e_{ii}\right)^2 + \mu\varepsilon^e_{ij}\varepsilon^e_{ij} + \mu k \ln\frac{1}{1-\frac{|\beta_{,y}||\sin\varphi|}{b\rho_s}}, \tag{6}$$

where μ and λ are Lamé constants, ρ_s the saturated dislocation density, and k a material constant. The first and second term of (6) describe the elastic energy, the third term is the energy of the dislocation network. With (5) and (6), the total energy functional becomes

$$E(u,v,\beta) = aL\int_0^h \left[\frac{1}{2}\lambda v_{,y}^2 + \frac{1}{2}\mu(u_{,y} - \beta\cos 2\varphi)^2 + \frac{1}{4}\mu\beta^2\sin^2 2\varphi \right.$$
$$\left. +\mu(v_{,y} - \frac{1}{2}\beta\sin 2\varphi)^2 + \mu k\ln\frac{1}{1-\frac{|\beta_{,y}||\sin\varphi|}{b\rho_s}}\right]\mathrm{d}y. \tag{7}$$

Functional (7) can be reduced to a functional depending on $\beta(y)$ only. Indeed, by first fixing $\beta(y)$ and taking the variation of (7) with respect to u and v, we derive the equilibrium equations

$$\mu(u_{,yy} - \beta_{,y}\cos 2\varphi) = 0,$$

$$(\lambda + 2\mu)v_{,yy} - \mu\beta_{,y}\sin 2\varphi = 0.$$

Integrating these equations and using the boundary conditions (1), we get

$$\begin{aligned} u_{,y} &= \gamma + (\beta - \langle\beta\rangle)\cos 2\varphi, \\ v_{,y} &= \kappa(\beta - \langle\beta\rangle)\sin 2\varphi, \end{aligned} \tag{8}$$

where $\kappa = \frac{\mu}{\lambda+2\mu}$, and $\langle\beta\rangle = \frac{1}{h}\int_0^h \beta\mathrm{d}y$. Substituting (8) into (7) and collecting the common terms, we obtain the energy functional in terms of β

$$E(\beta) = aL\int_0^h \mu\left[\frac{1}{2}(1-\kappa)\beta^2\sin^2 2\varphi + \frac{1}{2}\kappa\langle\beta\rangle^2\sin^2 2\varphi \right.$$
$$\left. +\frac{1}{2}(\gamma - \langle\beta\rangle\cos 2\varphi)^2 + k\ln\frac{1}{1-\frac{|\beta_{,y}||\sin\varphi|}{b\rho_s}}\right]\mathrm{d}y. \tag{9}$$

If the dissipation is negligible, then the plastic distortion β minimizes (9) under the constraint (3). The overall shear strain γ is regarded as a given function of time (control parameter), so one can study the evolution of the dislocation network which accompanies the change of γ.

If the resistance to dislocation motion cannot be neglected, then the energy minimization must be replaced by the flow rule. In case of the rate-independent plasticity, the flow rule for $\dot\beta \neq 0$ reads [6]

$$\frac{\partial D}{\partial\dot\beta} = -\frac{\delta_\gamma U}{\delta\beta}, \tag{10}$$

where the dissipation potential is

$$D = K|\dot\beta|,$$

with K being a positive constant called critical resolve shear stress, and the dot above a function denoting its time derivative. The right-hand side of (10) is the negative variational derivative of the energy with respect to β at fixed overall strain γ

$$\varkappa \equiv -\frac{\delta_\gamma U}{\delta\beta} = -\frac{\partial U}{\partial\beta} + \frac{\partial}{\partial y}\frac{\partial U}{\partial\beta_{,y}}.$$

For $\dot\beta = 0$, the evolution Eq. (10) does not have to be satisfied: it is replaced by the equation $\dot\beta = 0$.

For small up to moderate dislocation densities the logarithmic term in (9) may be approximated by the formula

$$\ln\frac{1}{1-\frac{|\beta_{,y}||\sin\varphi|}{b\rho_s}} \cong \frac{|\beta_{,y}||\sin\varphi|}{b\rho_s} + \frac{1}{2}\frac{\beta_{,y}^2\sin^2\varphi}{(b\rho_s)^2},$$

so that

$$E(\beta) = aL\int_0^h \mu\left[\frac{1}{2}(1-\kappa)\beta^2\sin^2 2\varphi + \frac{1}{2}\kappa\langle\beta\rangle^2\sin^2 2\varphi \right.$$
$$\left. + \frac{1}{2}(\gamma - \langle\beta\rangle\cos 2\varphi)^2 + k\left(\frac{|\beta_{,y}||\sin\varphi|}{b\rho_s} + \frac{1}{2}\frac{\beta_{,y}^2\sin^2\varphi}{(b\rho_s)^2}\right)\right]\mathrm{d}y. \tag{11}$$

We shall deal further only with this functional.

3 Dislocation nucleation at zero resistance

In the case of zero resistance (and, hence the energy dissipation is zero), the determination of $\beta(y)$ reduces to the minimization of the total energy (11). Since U is convex with respect to β and $\beta_{,y}$, the variational problem has a unique solution. It is convenient to introduce the dimensionless quantities

$$\bar E = \frac{b\rho_s}{aL\mu}E, \quad \bar y = yb\rho_s, \quad \bar h = hb\rho_s.$$

The dimensionless variable $\bar y$ changes on the interval $(0, \bar h)$. The functional (11) reduces to

$$E(\beta) = \int_0^h \left[\frac{1}{2}(1-\kappa)\beta^2\sin^2 2\varphi + \frac{1}{2}\kappa\langle\beta\rangle^2\sin^2 2\varphi \right.$$
$$\left. + \frac{1}{2}(\gamma - \langle\beta\rangle\cos 2\varphi)^2 + k|\beta'||\sin\varphi| + \frac{1}{2}k\beta'^2\sin^2\varphi\right]\mathrm{d}y, \tag{12}$$

where the prime denotes differentiation with respect to $\bar y$, and, for short, the bars over E, y, and h are dropped. We minimize functional (12) among functions satisfying the boundary conditions

$$\beta(0) = \beta(h) = 0. \tag{13}$$

We know that, for the variational problem of this type, there exists a threshold value γ_{en} such that when $\gamma < \gamma_{\mathrm{en}}$ no dislocations are nucleated and $\beta = 0$ [15]. Near the threshold value the dislocation density must be small so that the last term in (12) can be neglected. Besides, the width of the boundary layer tends to zero as $\gamma \to \gamma_{\mathrm{en}}$. This gives us the idea of finding the threshold value by employing the minimizing sequence of the form

$$\beta = \begin{cases} \frac{\beta_m}{\epsilon}y, & \text{for } y \in (0,\epsilon), \\ \beta_m, & \text{for } y \in (\epsilon, h-\epsilon), \\ \frac{\beta_m}{\epsilon}(h-y), & \text{for } y \in (h-\epsilon, h), \end{cases} \tag{14}$$

where β_m is an unknown constant, and ϵ is a small unknown length which tends to zero as $\gamma \to \gamma_{\text{en}}$. Substituting (14) into the energy functional (12) (with the last term being removed) and neglecting all small terms of order ϵ and higher, we obtain

$$E(\beta_m) = \frac{1}{2}[(\gamma - \beta_m \cos 2\varphi)^2 + \beta_m^2 \sin^2 2\varphi]h + 2k\,|\beta_m \sin\varphi|\,. \tag{15}$$

A rather simple analysis shows that the minimum of (15) is achieved at $\beta_m \neq 0$ if and only if

$$\gamma > \gamma_{\text{en}} = \frac{2k|\sin\varphi|}{h|\cos 2\varphi|},$$

otherwise it is achieved at $\beta_m = 0$ (no dislocations are nucleated). Note that the sign of β_m depends on the angle φ: β_m is positive if $0^\circ < \varphi < 45^\circ$ and is negative if $45^\circ < \varphi < 90^\circ$. In terms of the original length h the energetic threshold value reads

$$\gamma_{\text{en}} = \frac{2k}{hb\rho_s}\frac{|\sin\varphi|}{|\cos 2\varphi|},$$

showing clearly the size effect.

Due to the boundary conditions β' should change its sign on the interval $(0, h)$. The one-dimensional theory of dislocation pile-ups [16] as well as the solution of the analogous anti-plane shear problem [15] suggest to seek the minimizer in the form

$$\beta(y) = \begin{cases} \beta_1(y), & \text{for } y \in (0, l), \\ \beta_m, & \text{for } y \in (l, h-l), \\ \beta_1(h-y), & \text{for } y \in (h-l, h), \end{cases} \tag{16}$$

where β_m is a constant, l an unknown length, $0 \le l \le \frac{h}{2}$, and $\beta_1(l) = \beta_m$. We have to find $\beta_1(y)$ and the constants, β_m and l. With β from (16) the total energy functional becomes

$$\begin{aligned} E = 2\int_0^l \left[\frac{1}{2}(1-\kappa)\beta_1^2 \sin^2 2\varphi + k|\beta_1'||\sin\varphi| + \frac{1}{2}k\beta_1'^2 \sin^2\varphi\right] \mathrm{d}y \\ + \frac{1}{2}(1-\kappa)\beta_m^2 \sin^2 2\varphi(h-2l) + \frac{1}{2}h\big[\kappa\langle\beta\rangle^2 \sin^2 2\varphi + (\gamma - \langle\beta\rangle\cos 2\varphi)^2\big], \end{aligned} \tag{17}$$

where

$$\langle\beta\rangle = \frac{1}{h}\left(2\int_0^l \beta_1\,\mathrm{d}y + (h-2l)\beta_m\right). \tag{18}$$

Varying the energy functional (17) with respect to β_1 we obtain

$$-k\beta_1'' \sin^2\varphi + (1-\kappa)\beta_1 \sin^2 2\varphi + (\cos^2 2\varphi + \kappa \sin^2 2\varphi)\langle\beta\rangle - \gamma\cos 2\varphi = 0, \tag{19}$$

where $\beta_1(y)$ is subject to the boundary conditions

$$\beta_1(0) = 0, \quad \beta_1(l) = \beta_m. \tag{20}$$

The variation of (17) with respect to l gives an additional boundary condition at $y = l$

$$\beta_1'(l) = 0, \tag{21}$$

which means that the dislocation density must be continuous. Varying the energy functional with respect to β_m, we obtain a condition for β_m

$$2k|\sin\varphi|(\operatorname{sign}\beta_1') + [(\cos^2 2\varphi + \kappa\sin^2 2\varphi)\langle\beta\rangle - \gamma\cos 2\varphi + (1-\kappa)\beta_m \sin^2 2\varphi](h-2l) = 0. \tag{22}$$

Equations (19), $(20)_1$, and (21) yield the solution

$$\beta_1 = \beta_{1p}\,(1 - \cosh\eta y + \tanh\eta l \sinh\eta y)\,, \quad 0 \le y \le l \tag{23}$$

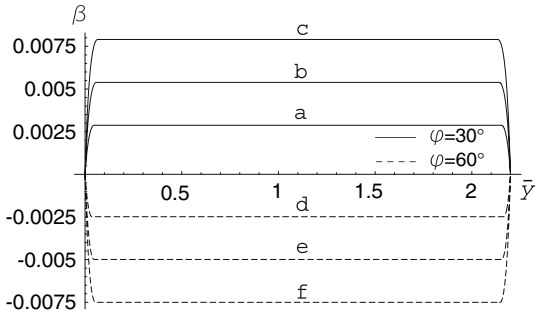

Fig. 2 Evolution of β: *a*, *d*) $\gamma = 0.0068$, *b*, *e*) $\gamma = 0.0118$, *c*, *f*) $\gamma = 0.0168$

with

$$\beta_{1p} = \frac{\gamma \cos 2\varphi - (\cos^2 2\varphi + \kappa \sin^2 2\varphi)\langle\beta\rangle}{(1-\kappa)\sin^2 2\varphi}, \tag{24}$$

and

$$\eta = 2\sqrt{\frac{1-\kappa}{k}}|\cos\varphi|.$$

With (18), $(20)_2$, (23), and (24), we obtain the average of β

$$\langle\beta\rangle = \frac{\gamma\cos 2\varphi\left[2\left(l - \frac{\tanh\eta l}{\eta}\right) + \left(1 - \frac{1}{\cosh\eta l}\right)(h-2l)\right]}{g(l)}, \tag{25}$$

where

$$g(l) = h(1-\kappa)\sin^2 2\varphi + (\cos^2 2\varphi + \kappa\sin^2 2\varphi)\left[2\left(l - \frac{\tanh\eta l}{\eta}\right) + \left(1 - \frac{1}{\cosh\eta l}\right)(h-2l)\right],$$

and

$$\beta_m = \frac{\gamma\cos 2\varphi - \langle\beta\rangle(\cos^2 2\varphi + \kappa\sin^2 2\varphi)}{(1-\kappa)\sin^2 2\varphi}\left(1 - \frac{1}{\cosh\eta l}\right). \tag{26}$$

Substitution of (26) into (22) gives the following equation to determine l

$$f(l) \equiv 2k|\sin\varphi|(\mathrm{sign}\beta_1') - \frac{\gamma\cos 2\varphi - \langle\beta\rangle(\cos^2 2\varphi + \kappa\sin^2 2\varphi)}{\cosh\eta l}(h-2l) = 0.$$

Figure 2 shows the evolution of $\beta(\bar{y})$ as γ increases for $\varphi = 30°$ (continuous lines) and $\varphi = 60°$ (dashed lines), where $\bar{y} = yb\rho_s$. For the numerical simulation we took $k = 1.138 \times 10^{-3}$, $\rho_s = 8.8 \times 10^{15}\,\mathrm{m}^{-2}$, $\mu = 26.3$ GPa, $\nu = 0.33$, $b = 2.5 \times 10^{-10}$ m, $h = 10^{-6}$ m, so that $\bar{h} = hb\rho_s = 2.2$.

It is interesting to plot the shear stress $\tau = \mu(\gamma - \langle\beta\rangle\cos 2\varphi)$ as function of the shear strain. As we know, for $\gamma < \gamma_{\mathrm{en}}$ no dislocations are nucleated and $\beta = 0$, so the shear stress $\tau = \mu\gamma$. For $\gamma > \gamma_{\mathrm{en}}$, we take $\langle\beta\rangle$ from (25) to compute the shear stress.

Figure 3 shows the normalized shear stress versus shear strain curve OAB for $\varphi = 30°$ and OA′B′ for $\varphi = 60°$. There is a "work hardening" section AB for $\gamma > \gamma_{\mathrm{en}}$ caused by the dislocation pile-up. Mention, however, that there is no residual strain as we unload the crystal by decreasing γ: the stress–strain curve follows the same path BAO, so the plastic deformation is completely reversible, and no energy dissipation occurs. In the course of unloading the dislocations nucleated annihilate, and as we approach the point A they all disappear.

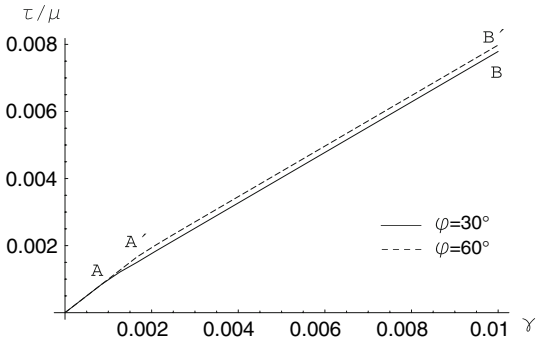

Fig. 3 Normalized shear stress versus shear strain curve

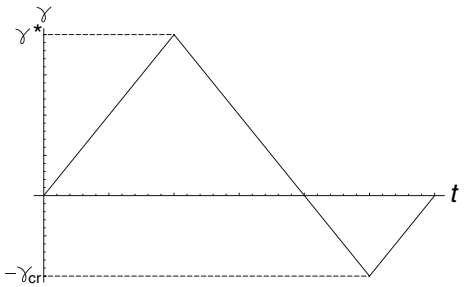

Fig. 4 A closed loading path

4 Plastic distortion at non-zero resistance

If the resistance to dislocation motion (and hence the dissipation) cannot be neglected, the plastic distortion may evolve only if the yield condition $|\varkappa| = K$ is fulfilled. If $|\varkappa| < K$, then β is frozen, the dislocation density remains unchanged and the crystal deforms elastically. Computing the variational derivative of (11), we derive from (10) the yield condition

$$\mu \left| k\frac{\beta_{,yy}\sin^2\varphi}{b^2\rho_s^2} - (1-\kappa)\beta\sin^2 2\varphi - (\cos^2 2\varphi + \kappa\sin^2 2\varphi)\langle\beta\rangle + \gamma\cos 2\varphi \right| = K.$$

Consider first the case $\varphi < 45°$. We divide this equation by μ and introduce the dimensionless variable $\bar{y} = yb\rho_s$ to transform the yield condition to

$$\left|k\beta''\sin^2\varphi - (1-\kappa)\beta\sin^2 2\varphi - (\cos^2 2\varphi + \kappa\sin^2 2\varphi)\langle\beta\rangle + \gamma\cos 2\varphi\right| = \gamma_{\rm cr}\cos 2\varphi, \tag{27}$$

with $\gamma_{\rm cr} \equiv K/\mu\cos 2\varphi$ and the prime denoting the derivative with respect to $\bar{y}$. We shall further omit the bar over y for short.

We regard γ as a given function of time (the driving variable) and try to determine $\beta(t, y)$. We consider the following loading path: γ is first increased from zero to some value $\gamma^* > \gamma_{\rm cr}$, then decreased to $-\gamma_{\rm cr}$, and finally increased to zero as shown in Fig. 4. The rate of change of $\gamma(t)$ does not affect the results due to the rate independence of dissipation. The problem is to determine the evolution of β as function of t and y, provided $\beta(0, y) = 0$ and $\varphi < 45°$.

Since the plastic distortion, β, is initially zero, we see from (27) that $\beta = 0$ as long as $\gamma < \gamma_{\rm cr}$. Thus, the dissipative threshold stress (the yield stress) $\tau_y = K/\cos 2\varphi$ in this case. For small $\beta(t, x)$ and $\gamma > \gamma_{\rm cr}$, the yield condition becomes

$$k\beta''\sin^2\varphi - (1-\kappa)\beta\sin^2 2\varphi - (\cos^2 2\varphi + \kappa\sin^2 2\varphi)\langle\beta\rangle + \gamma\cos 2\varphi = \gamma_{\rm cr}\cos 2\varphi, \tag{28}$$

Let us introduce the deviation of $\gamma(t)$ from the critical shear $\gamma_{\rm cr}$, $\gamma_r = \gamma - \gamma_{\rm cr}$ and simplify (28) to obtain

$$k\beta''\sin^2\varphi - (1-\kappa)\beta\sin^2 2\varphi - (\cos^2 2\varphi + \kappa\sin^2 2\varphi)\langle\beta\rangle + \gamma_r\cos 2\varphi = 0.$$

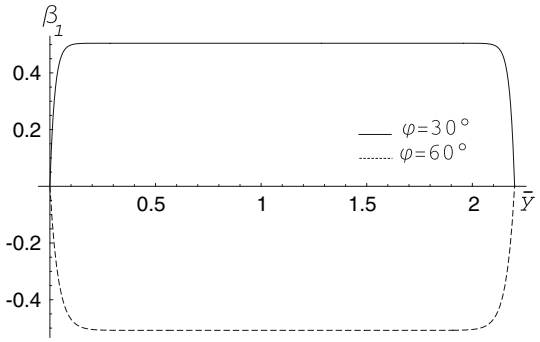

Fig. 5 Graphs of $\beta_1(\bar{y})$

Since this equation is linear, β is proportional to γ_r such that $\beta = \gamma_r \beta_1$, where β_1 is the solution of the following equation

$$k\beta_1'' \sin^2\varphi - (1-\kappa)\beta_1 \sin^2 2\varphi - (\cos^2 2\varphi + \kappa \sin^2 2\varphi)\langle\beta_1\rangle + \cos 2\varphi = 0. \tag{29}$$

The analogous problem of anti-plane shear at nonzero resistance [15] suggests that the solution of (29) is symmetric, i.e.,

$$\beta_1(y) = \beta_1(h-y) \quad \text{for } y \in (h/2, h). \tag{30}$$

Function $\beta_1(y)$ is determined from Eq. (29) and the boundary conditions

$$\beta_1(0) = 0, \quad \beta_1'(h/2) = 0. \tag{31}$$

The first condition means that dislocations cannot reach the boundary of the region because of the prescribed displacement. The second condition follows from the continuity of plastic distortion and the symmetry property (30).

Equations (29) and (31) admit the solution

$$\beta_1 = \beta_{1p}\left(1 - \cosh\eta y + \tanh\eta\frac{h}{2}\sinh\eta y\right), \quad 0 \le y \le \frac{h}{2}, \tag{32}$$

with

$$\beta_{1p} = \frac{\cos 2\varphi - (\cos^2 2\varphi + \kappa \sin^2 2\varphi)\langle\beta_1\rangle}{(1-\kappa)\sin^2 2\varphi}, \tag{33}$$

and

$$\eta = 2\sqrt{\frac{1-\kappa}{k}}|\cos\varphi|. \tag{34}$$

The average of β_1 is obtained in the form

$$\langle\beta_1\rangle = \frac{\cos 2\varphi\left(1 - \frac{2\tanh\eta\frac{h}{2}}{\eta h}\right)}{(1-\kappa)\sin^2 2\varphi + (\cos^2 2\varphi + \kappa\sin^2 2\varphi)\left(1 - \frac{2\tanh\eta\frac{h}{2}}{\eta h}\right)}. \tag{35}$$

Figure 5 shows the graphs of $\beta_1(\bar{y})$ for $\varphi = 30°$ (continuous line) and $\varphi = 60°$ (dashed line). For the numerical simulation we took $\mu = 26.3$ GPa, $\nu = 0.33$, $k = 1.138\times10^{-3}$, $\rho_s = 8.8\times10^{15}\,\mathrm{m}^{-2}$, $b = 2.5\times10^{-10}$ m, $\gamma_{\mathrm{cr}} = \gamma_{\mathrm{en}}$, and $h = 1\mu$m, so that $\bar{h} = hb\rho_s = 2.2$.

After reaching $\gamma^* > \gamma_{\mathrm{cr}}$, we unload the crystal by decreasing γ. Since $\varkappa$ becomes smaller than K, β does not change ($\beta = \beta^*(y)$) until

$$k\beta^{*\prime\prime}\sin^2\varphi - (1-\kappa)\beta^*\sin^2 2\varphi - (\cos^2 2\varphi + \kappa\sin^2 2\varphi)\langle\beta^*\rangle + \gamma\cos 2\varphi = -\gamma_{\mathrm{cr}}\cos 2\varphi, \tag{36}$$

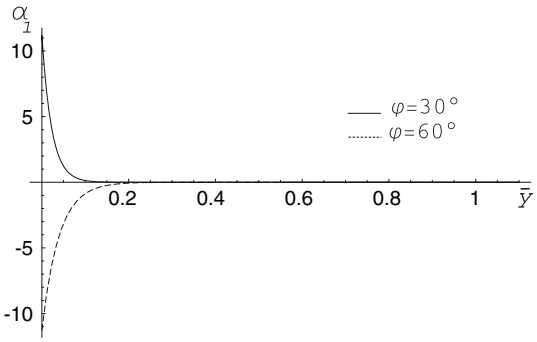

Fig. 6 Graphs of $\alpha_1(\bar{y})$

where $\beta^*(y)$ is the solution of (28) for $\gamma(t) = \gamma^*$. From (36) we can see that the plastic flow begins when $\gamma - (\gamma^* - \gamma_{\rm cr}) = -\gamma_{\rm cr}$, i.e., for $\gamma = \gamma_* = \gamma^* - 2\gamma_{\rm cr}$. From that value of γ, the yield condition $\varkappa = -K$ takes place leading to the decrease of β which should be now determined by the equation

$$k\beta'' \sin^2\varphi - (1-\kappa)\beta \sin^2 2\varphi - (\cos^2 2\varphi + \kappa \sin^2 2\varphi)\langle\beta\rangle + \gamma \cos 2\varphi = -\gamma_{\rm cr} \cos 2\varphi, \tag{37}$$

Since for $\gamma \in (-\gamma_{\rm cr}, \gamma_*)$, the deviation $\gamma_l = \gamma + \gamma_{\rm cr}$ is positive, Eq. (37) can again be transformed to Eq. (29) and solved in exactly the same manner if we replace $\gamma_r = \gamma - \gamma_{\rm cr}$ in all formulae (32)–(35) by $\gamma_l = \gamma + \gamma_{\rm cr}$. As γ approaches $-\gamma_{\rm cr}$, β tends to zero because $\gamma_l \to 0$. The further increase of γ from $-\gamma_{\rm cr}$ to zero does not cause change in β which remains zero.

It is not difficult to modify the construction given above to find the solution for $\varphi > 45°$.

5 Dislocation density and stress–strain curve

The normalized dislocation density $\alpha = \beta_{,y} \sin\varphi$ can be calculated from the solution (32). Since $\beta(y)$ is proportional to γ_r, $\alpha(y)$ is also proportional to γ_r such that $\alpha(y) = \gamma_r \alpha_1(y)$. For $y \in (0, h/2)$ we have

$$\alpha_1(y) = \beta_{1p}\left(-\eta \sinh \eta y + \eta \cosh \eta y \tanh \frac{\eta h}{2}\right) \sin\varphi,$$

with β_{1p} from (33) and η from (34). For $y \in (h/2, h)$ we have $\alpha_1(y) = -\alpha_1(h-y)$ due to symmetry. Figure 6 shows the graphs of α_1 for $\varphi = 30°$ (continuous line) and $\varphi = 60°$ (dashed line) for $y \in (0, h/2)$.

It is interesting to calculate the shear stress τ which is a measurable quantity. During the loading, we have for the normalized shear stress (or the elastic shear strain)

$$\gamma^e = \frac{\tau}{\mu} = \gamma_{\rm cr} + \left(\gamma_r - \left(1 - \frac{2\tanh\frac{\eta h}{2}}{\eta h}\right)\beta_{1p} \cos 2\varphi\right), \tag{38}$$

with β_{1p} from (33). The second term of (38) causes the hardening due to the dislocations pile-up. Equation (38) describes the size effect in this model.

Figure 7 shows the comparison between the stress–strain curves during the loading obtained from energy minimization, from (38), and from the discrete dislocation simulations reported in [11,12]. In order to compare with the discrete dislocation simulations we took $\varphi = 60°$, $\tau_0 = 1.9 \times 10^{-3}\mu$m and let all other material constants remain the same as in the previous simulations. The stress–strain curves in the discrete dislocation simulations are provided for three different ratios h/d, where d is the spacing between the active slip planes. Both curves obtained from energy minimization as well as from the flow rule nearly coincide with each other and show good agreement with the discrete dislocation simulations for $h/d = 80$.

Figure 8 shows the comparison between the total shear strain profiles obtained from energy minimization, from the flow rule, and from the discrete dislocation simulations reported in [11,12]. Both profiles obtained from energy minimization and from the flow rule again show good agreement with the discrete dislocation simulations for $h/d = 80$.

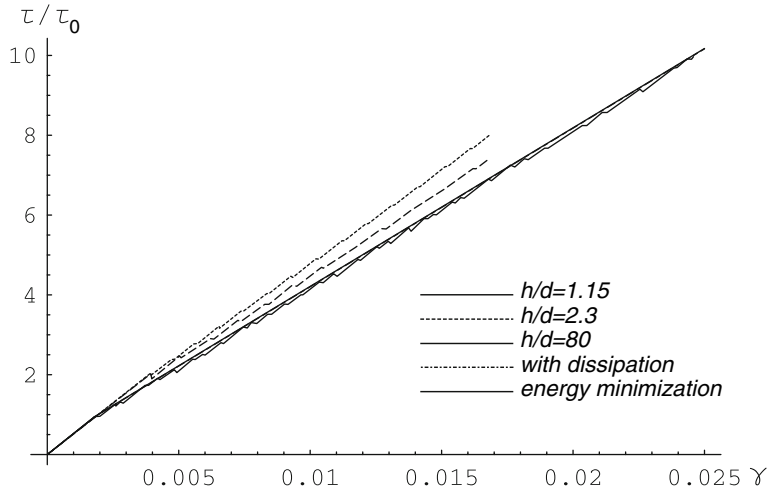

Fig. 7 The normalized shear stress versus shear strain curve

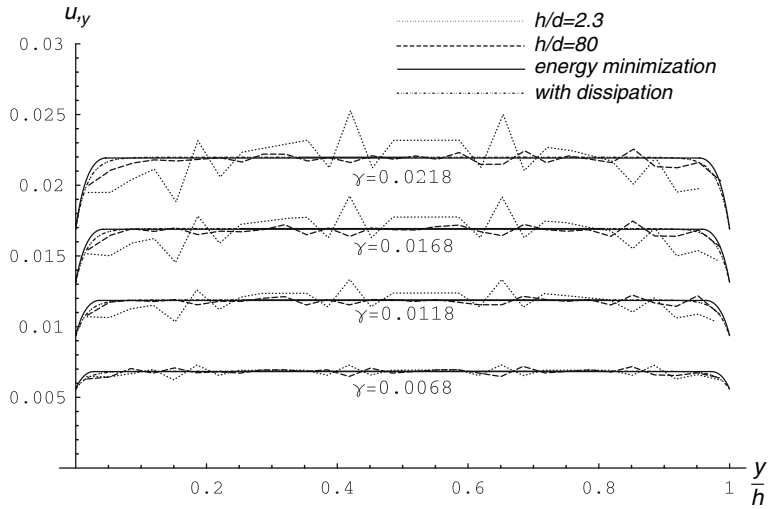

Fig. 8 The total shear strain profile

During the inverse loading, when the yield condition $\varkappa = -K$ holds true, Eq. (38) changes to

$$\frac{\tau}{\mu} = -\gamma_{\rm cr} + \left(\gamma_l - \left(1 - \frac{2\tanh\frac{\eta h}{2}}{\eta h}\right)\beta_{1p}\cos 2\varphi\right),$$

with the deviation $\gamma_l = \gamma + \gamma_{\rm cr}$ used instead of $\gamma_r = \gamma - \gamma_{\rm cr}$ for the average of β.

Figure 9 shows the normalized shear stress (or elastic shear strain) versus shear strain curve for the loading path of Fig. 4, with $\gamma^* = 0.01$, $\varphi = 60°$, while all other parameters remain the same. The straight line OA corresponds to the purely elastic loading with γ increasing from zero to $\gamma_{\rm cr}$. Line AB corresponds to the plastic yielding with $\varkappa = K$. Yielding begins at point A with the yield stress $\tau_y = -K/\cos 2\varphi$, and we can observe the work hardening due to the dislocation pile-up which is described by the second term of (38). During the unloading as γ decreases from γ^* to $\gamma_* = \gamma^* - 2\gamma_{\rm cr}$ (line BC) the plastic distortion $\beta = \beta^*$ is frozen. As γ decreases further from γ_* to $-\gamma_{\rm cr}$, the plastic yielding occurs with $\varkappa = -K$ (line CD). From Fig. 9, it is seen that the yield stress $\tau_y = \tau^* + 2K/\cos 2\varphi$ at point C, at which the inverse plastic flow sets on, is larger than $-K/\cos 2\varphi$ (because $\tau^* > -K/\cos 2\varphi$). Along line CD, as γ is decreased, the created dislocations annihilate, and at point D all dislocations have disappeared. Finally, as γ increases from $-\gamma_{\rm cr}$ to zero, the crystal behaves elastically with $\beta = 0$. In this closed cycle OABCDO dissipation occurs only on lines AB and CD. It is interesting that lines DA and BC are parallel and have the same length. In phenomenological

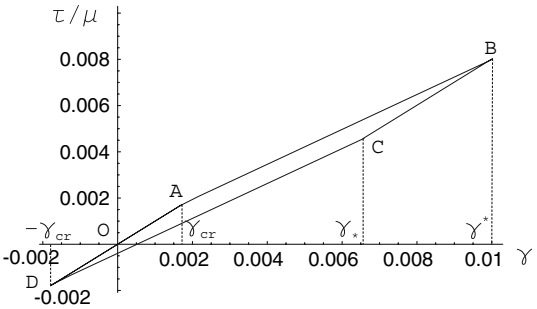

Fig. 9 Normalized shear stress versus shear strain curve for $\varphi = 60^\circ$

plasticity theory this property is modeled as the translational shift of the yield surface in the stress space, the so-called Bauschinger effect.

6 Conclusion

We have shown in this paper that the plane-strain constrained shear problem can be analytically solved within the continuum dislocation theory. If the resistance to dislocation motion is negligible and only one slip system is active, there is the energetic threshold stress for the dislocation nucleation that depends on the slip direction. The stress–strain curve is completely reversible and no energy dissipation occurs. The work hardening caused by the dislocation pile-up and the threshold stress are inversely proportional to the size of specimen times the saturated dislocation density.

If the resistance to dislocation motion is taken into account, then the stress–strain curve becomes a hysteresis loop. The work hardening and the Bauschinger effect are quantitatively described in terms of the dislocation density, and the size effect can be observed. The comparison with the discrete dislocation simulation shows good agreement between the continuum and discrete approaches.

References

1. Nye, J.F.: Some geometrical relations in dislocated crystals. Acta Metall. **1**, 153–162 (1953)
2. Kondo, K.: On the geometrical and physical foundations of the theory of yielding. In: Proceedings 2. Japan Congr. Appl. Mech. pp 41–47 (1952)
3. Bilby, B.A., Bullough, R., Smith, E.: Continuous distributions of dislocations: a new application of the methods of non-Riemannian geometry. Proc. R. Soc. Lond. **A231**, 263–273 (1955)
4. Kröner, E.: Kontinuumstheorie der Versetzungen und Eigenspannungen. Springer, Berlin (1958)
5. Berdichevsky, V.L., Sedov, L.I.: Dynamic theory of continuously distributed dislocations. Its relation to plasticity theory. J. Appl. Math. Mech. (PMM) **31**, 989–1006 (1967)
6. Berdichevsky, V.L.: Continuum theory of dislocations revisited. Contin. Mech. Thermodyn. **18**, 195–222 (2006)
7. Ortiz, M., Repetto, E.A.: Nonconvex energy minimization and dislocation structures in ductile single crystals. J. Mech. Phys. Solids **47**, 397–462 (1999)
8. Berdichevsky, V.L.: Homogenization in micro-plasticity. J. Mech. Phys. Solids **53**, 2457–2469 (2005)
9. Berdichevsky, V.L.: On thermodynamics of crystal plasticity. Scripta Mater. **54**, 711–716 (2006)
10. Acharya, A., Basani, J.L.: Incompatibility and crystal plasticity. J. Mech. Phys. Solids **48**, 1565–1595 (2000)
11. Needleman, A., Van der Giessen, E.: Discrete dislocation and continuum descriptions of plastic flow. Mater. Sci. Eng. **A309**(310), 1–13 (2001)
12. Shu, J.Y., Fleck, N.A., Van der Giessen, E., Needleman, A.: Boundary layers in constrained plastic flow: comparison of nonlocal and discrete dislocation plasticity. J. Mech. Phys. Solids **49**, 1361–1395 (2001)
13. Groma, I., Csikor, F., Zaiser, M.: Spatial correlations and higher-order gradient terms in a continuum description of dislocation dynamics. Acta Mater. **51**, 1271–1281 (2003)
14. Huang, Y., Hwang, Q.S., Li, K.C., Gao, H.: A conventional theory of mechanism-based strain gradient plasticity. J. Mech. Phys. Solids **20**, 753–782 (2004)
15. Berdichevsky, V.L., Le, K.C.: Dislocation nucleation and work hardening in anti-planed constrained shear. Contin. Mech. Thermodyn. **18**, 455–467 (2007)
16. Leibfried, G.: Verteilung von Versetzungen im statischen Gleichgewicht. Z. Phys. **130**, 214–226 (1951)